JOURNAL OF CATALYSIS **179,** 258–266 (1998)
ARTICLE NO. CA982201

Transition Metal Oxide Catalyzed Carbon Black Oxidation: A Study with $^{18}O_2$

Guido Mul,*,[1] Freek Kapteijn,*,[2] Ciska Doornkamp,† and Jacob A. Moulijn*

*Industrial Catalysis, Delft University of Technology, Julianalaan 136, 2628 BL Delft, The Netherlands; and †Gorlaeus Laboratories, Leiden University, P.O. Box 9502, 2300 RA Leiden, The Netherlands

Received March 10, 1998; revised June 9, 1998; accepted June 9, 1998

Physical mixtures of carbon black and several transition metal oxides (Cr_2O_3, Co_3O_4, Fe_2O_3, MoO_3, V_2O_5, and K_2MoO_4) were treated batchwise in $^{18}O_2$ at 625–675 K in a high-vacuum batch reactor. Three reaction mechanisms are proposed to be operative in the catalyzed oxidation of carbon black. The isotopic reaction product composition ($C^{16}O$, $C^{18}O$, $C^{16}O_2$, $C^{16}O^{18}O$, and $C^{18}O_2$) in experiments, in which $^{18}O_2$ and $^{16}O_2$ were fed alternately, showed that the amount of gas-phase oxygen incorporated in the products decreases in the series $Cr_2O_3 > Co_3O_4 = Fe_2O_3 > MoO_3 > V_2O_5 > K_2MoO_4$. Based on this trend, a surface redox mechanism is proposed for Cr_2O_3, Co_3O_4, and Fe_2O_3 catalyzed carbon black oxidation in which only surface oxygen (lattice oxygen of the oxide located in the surface layer) participates. Considering the formation of carbon surface oxygen complexes, and the relatively high fraction of ^{18}O-labeled products obtained for Cr_2O_3/carbon black mixtures, a spill-over mechanism, involving adsorbed surface oxygen, is suggested to run in parallel with the surface redox mechanism for Cr_2O_3. A "classical" redox mechanism, in which lattice oxygen from the bulk of the oxide is active, is proposed for MoO_3, V_2O_5, and K_2MoO_4. Significant carbothermic reduction of MoO_3 and V_2O_5 was observed in the absence of gas-phase oxygen. For K_2MoO_4 gas-phase oxygen is needed to keep the reaction going, although the highest amount of ^{16}O-labeled products was obtained. K_2MoO_4 is not carbothermally reduced at the temperatures used. A "push–pull" mechanism seems to be operative for K_2MoO_4. Oxygen spill-over might also occur in the MoO_3-, V_2O_5-, and K_2MoO_4-catalyzed carbon black oxidation, in view of the formation of carbon surface oxygen complexes, but this plays a minor role in the overall oxidation mechanism. © 1998 Academic Press

Key Words: **carbon black; catalytic oxidation; $^{18}O_2$; spill-over; mechanism.**

INTRODUCTION

Numerous mechanistic studies on transition metal oxide catalyzed oxidation reactions have already been performed. Altogether, four oxidation mechanisms have been proposed for the range of 625–750 K: a redox (Mars and van Krevelen) mechanism (1,2); a push-pull mechanism, e.g. (3,4); an associative (Langmuir–Hinshelwood) mechanism (5,6); and a spill-over mechanism (7–9).

In the 1960s Winter found evidence for a redox mechanism in the catalytic oxidation of CO by transition metal oxides, using labeled oxygen ($^{18}O_2$) (10–12). In the same period Novakova *et al.* (13), Boreskov (14), Popovski *et al.* (15), and Muzykantov *et al.* (16) used $^{18}O_2$ to study the exchange of gaseous oxygen with the oxide lattice for a large number of transition metal oxides and established the existence of various mechanisms of exchange. They found a correlation between the oxygen exchange activity and the activity of metal oxides in the oxidation of carbon monoxide, hydrogen, and methane. Keulks (17) demonstrated that lattice oxygen of bismuth molybdate was incorporated in acrolein formed by propene oxidation. Recently, Iizuka *et al.* (18–20) studied the mechanism of the MoO_3 catalyzed oxidation of CO using $^{18}O_2$ and also found evidence for a redox mechanism.

The push-pull mechanism is derived from the redox mechanism and has been proposed for catalytic CO oxidation on ZnO (3); CO is adsorbed on the ZnO surface, followed by CO_2 formation (with the incorporation of lattice oxygen) and its release, in combination with a simultaneous reoxidation of the active site. CO_2 is only formed in the presence of gaseous oxygen, while ZnO is not reduced by CO at temperatures where catalytic oxidation takes place. The existence of this mechanism can be simulated upon oxidation of CO on oxides that are very easily reduced. Then a small number of freshly reduced sites induce the reaction of CO with oxygen adsorbed on these newly created sites (21).

The associative mechanism involves the adsorption of both the reactant (e.g., CO) and oxygen on the surface of a catalyst (e.g., a transition metal oxide). Recombination of dissociated oxygen and CO results in CO_2 formation. The oxidized product only contains gas-phase oxygen, while lattice oxygen is not consumed.

Finally, oxidation reactions over combinations of two metal oxides have been explained by a spill-over mechanism. Oxygen is adsorbed and activated on one metal oxide (the donor) and transferred to the second metal oxide (the

[1] Present address: SRI-International, 333 Ravenswood Ave., Menlo Park, CA 94025.

[2] Corresponding author.

0021-9517/98 $25.00

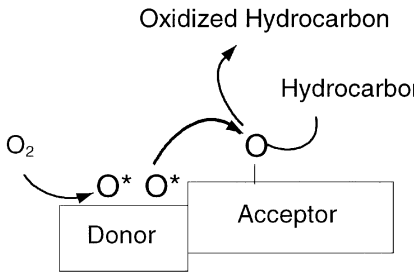

SCHEME 1. Representation of the "spill-over" mechanism, proposed to explain synergetic effects of metal oxides in selective oxidation reactions.

acceptor). The reactant (e.g., a hydrocarbon) reacts with the oxygen adsorbed on the acceptor (7–9) (See Scheme 1, where O* indicates activated oxygen).

Although catalytic carbon oxidation has been studied extensively, only a few studies describe details such as the mechanistic steps discussed above. The use of $^{18}O_2$ has so far been limited to a study on CaO catalyzed carbon oxidation (22–24). Nonetheless, several authors have proposed a redox mechanism for the catalytic oxidation of carbonaceous materials by transition metal oxides such as activated carbon, single crystal graphite, and model soot particulate (25–27). McKee *et al.* (27) state that only if carbothermic reduction (i.e., reduction of the metal oxide by carbon) is thermodynamically feasible, a metal oxide can catalyze the oxidation of carbon. This tendency to suggest, based on bulk thermodynamic properties, one general mechanism operating with all transition metal oxides in the oxidation of carbon can be doubted, due to the observation that some metal oxides (V_2O_5, MoO_3, K_2MoO_4, Cr_2O_3) catalyze the formation of carbon surface oxygen complexes (SOCs), whereas others do not (Fe_2O_3, Co_3O_4) (28). Furthermore, quite different types of carbon black oxidation profiles were found to be strongly dependent on the transition metal oxide involved (29). Surface oxygen complexes (SOCs) at the carbon are proposed to be generated by oxygen spill-over (the carbon or carbon black surface acts as the acceptor). In order to explain several microscopic observations, Baker and Chludzinsky (30) also proposed such a spill-over mechanism for the Cr_2O_3 catalyzed carbon black oxidation, but this is one of the few exceptions, where the catalysed carbon oxidation is not explained by a redox mechanism.

In this paper a study on the reactivity of a carbonaceous material in $^{18}O_2$ is described, with the aim to reveal the mechanism of catalytic carbon black oxidation by various transition metal oxides and to explain their different behavior in SOC formation. This all relates to the catalytic oxidation of diesel soot (28,29).

EXPERIMENTAL

Fe_2O_3 and Co_3O_4 were prepared by thermal decomposition of the corresponding nitrates (Aldrich, 99%) in static air at 775 and 875 K, respectively. Cr_2O_3 was prepared by calcination of CrO_3 at 775 K and V_2O_5, by thermal decomposition of NH_4VO_3 at 675 K in static air. MoO_3 (Merck, *p.a.*) and K_2MoO_4 (Fluka >98%) were used as received. The BET surface area of the pure metal oxides, determined by N_2 adsorption at 77 K, was as follows: Fe_2O_3, 19 m^2g^{-1}; Cr_2O_3, 24 m^2g^{-1}; Co_3O_4, 22 m^2g^{-1}; V_2O_5, 6 m^2g^{-1}; MoO_3, $\approx$1 m^2g^{-1}; and K_2MoO_4, <1 m^2g^{-1}. Printex-U (BET-surface area: 96 m^2g^{-1}, Degussa) was used in this mechanistic study, as it does not contain any catalytically active species and has low N, O, and S content (29). A transition metal oxide was mixed with Printex-U in a weight ratio of 2 : 1 or 5 : 1 by milling in a ball-mill (1 h) in order to obtain "tight contact" conditions, needed for a reproducible carbon black oxidation activity (29,31). The milling speed and, more importantly, milling time were relatively low (32,33). Significant changes in BET surface area, X-Ray diffraction patterns, and DRIFT spectra of the metal oxides before and after milling were not observed (28,29). We cannot exclude, however, that defect structures have somewhat changed, as was observed for MoO_3 (33).

A high-vacuum system was used for the oxidation experiments, which was connected to a mass-spectrometer (VG Instruments MM8-80s) (21). M/e units in the range of 10–60 were analyzed every 2 min. Sample sizes of 23 mg carbon black (12 mg for the 5 : 1 samples), and 47 mg metal oxide (58 mg for the 5 : 1 samples) were used and allowed to react in a quartz batch reactor of about 910 ml. The experimental procedure is outlined in Fig. 1. Outgassing of the sample was accomplished in about 1 h at room temperature in a vacuum. Subsequently, $^{16}O_2$ was introduced in the reactor also at room temperature (to prevent carbothermic reduction), followed by heating to the desired reaction temperature (625–700 K) at 5 K/min. $^{16}O_2$ and reaction products CO and CO_2, formed by decomposition of SOCs and reaction with $^{16}O_2$, were removed by evacuating the reactor for 15 min. Then, the first isothermal experiment was started by the introduction of 0.3 mbar $^{18}O_2$ in the reactor, corresponding to an amount consumed in about 30–60 min (depending on the catalytic activity). After every experiment the reactor was outgassed for another 15 min to remove reaction products, before the introduction of a new batch of $^{18}O_2$ (or $^{16}O_2$). Generally, two isothermal experiments

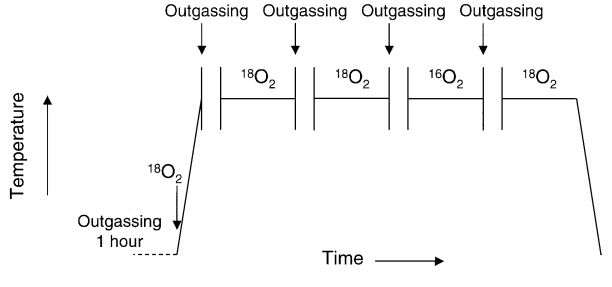

FIG. 1. Outline of the experimental procedure.

were performed in $^{18}O_2$, followed by one in $^{16}O_2$ and one in $^{18}O_2$, as indicated in Fig. 1. The intensity of the measured masses has not been corrected for CO_2 fragmentation as fluctuations occurred from measurement to measurement (34). Fragmentation was generally less than 5%. The isotopic ratio of labeled and unlabeled oxygen in the products CO and CO_2, referred to as IPR (isotopic product ratio), is defined in Eq. [1].

$$\mathrm{IPR} = \frac{\lfloor 2C^{18}O_2 + C^{18}O + C^{18}O^{16}O \rfloor}{[2C^{16}O_2 + C^{16}O + C^{18}O^{16}O]}. \qquad [1]$$

The IPR was calculated based on the relative m/e intensities directly, after all the $^{18}O_2$ had been converted. The amount of oxygen introduced in the batch reactor was relatively small, compared to both the amount of oxide and the amount of carbon; a carbon black conversion of only 1–2% was reached after four sequential batches of oxygen.

RESULTS

Uncatalyzed Carbon Black Oxidation

In general, labeled/unlabeled product distributions obtained in the metal oxide catalyzed carbon black oxidation might be affected by the uncatalyzed carbon black oxidation and carbon–oxygen complexes already present on the carbon black surface before the experiment. The oxidation pattern of carbon black at 650 K, without a catalyst, is shown in Fig. 2. The oxidation rate is rather low (compare, e.g., Fig. 3); 30–40% of the introduced amount of $^{18}O_2$ was converted within 1 h, whereas under the conditions of Fig. 3 this takes only 7 min. Although only $^{18}O_2$ and carbon black are introduced into the batch reactor, some ^{16}O labeled products (predominantly $C^{18}O^{16}O$) are formed, obviously due to decomposition of surface oxygen complexes (SOCs) originally present on the surface of Printex-U. In view of the low reaction rate, the contribution of the uncatalyzed carbon black oxidation to product distributions obtained in isothermal catalytic carbon black oxidation experiments is neglected.

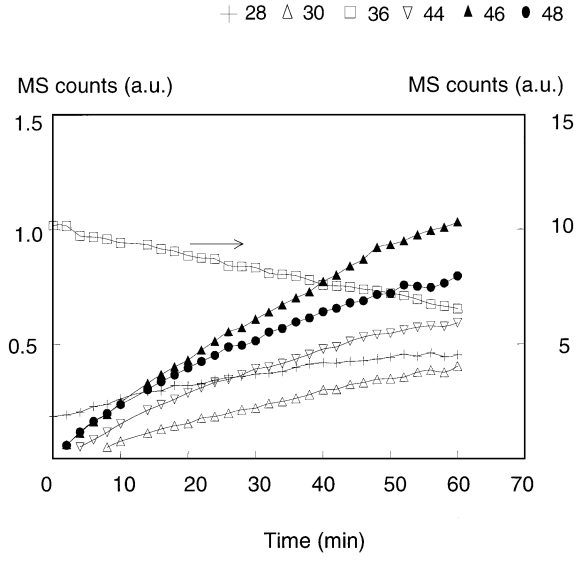

FIG. 2. First isothermal measurement performed with 25 mg pure carbon black in 0.3 mbar $^{18}O_2$. The development of the $C^{16}O$ (28), $C^{18}O$ (30), $^{18}O_2$ (36, right *y*-axis), $C^{16}O_2$ (44), $C^{16}O^{18}O$ (46), and $C^{18}O_2$ (48) concentrations at 650 K as a function of time are shown.

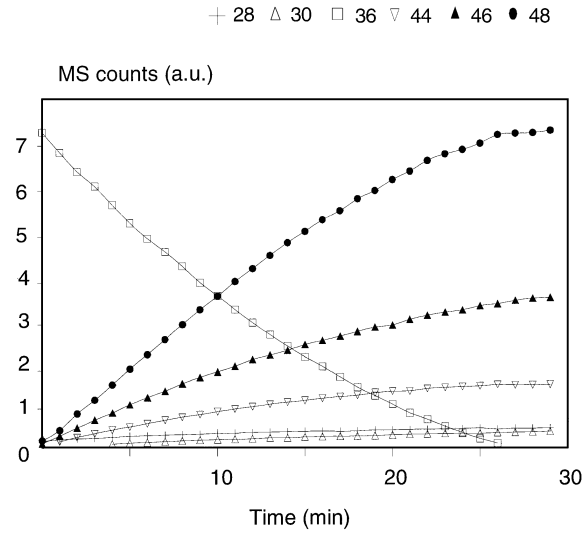

FIG. 3. Development of the $C^{16}O$ (28), $C^{18}O$ (30), $^{18}O_2$ (36), $C^{16}O_2$ (44), $C^{16}O^{18}O$ (46), and $C^{18}O_2$ (48) concentrations with time at 675 K. The first isothermal measurement, performed on 70 mg of a Cr_2O_3/carbon black mixture (2 : 1 mass ratio).

Cr_2O_3 and Fe_2O_3 Catalyzed Carbon Black Oxidation

A typical development of the product concentrations by reaction of a Cr_2O_3/carbon black sample at 675 K in $^{18}O_2$ is shown in Fig. 3. It takes less than 30 min to consume 0.3 mbar $^{18}O_2$ at 675 K. Besides $C^{18}O_2$ and $C^{18}O$, ^{16}O labeled compounds are also formed, of which the largest quantity is $C^{16}O^{18}O$. Once $^{18}O_2$ has completely reacted, CO and CO_2 are no longer produced; carbothermic reduction is not observed. Also, the isotopic distribution does not change any further. It is clear that oxygen exchange between $C^{18}O_2$ or $C^{18}O^{16}O$ and the oxide oxygen, if it occurs at all, is very slow, compared to the oxidation rate. This observation implies that a negligible contribution of the exchange reaction to the product distribution is expected.

In the subsequent (second) isothermal experiment performed with the Cr_2O_3/carbon black mixture in $^{18}O_2$, the IPR increased from 4.3 to 6. This suggests that some ^{18}O is stored in the sample during the first measurement performed in $^{18}O_2$, either on the carbon black surface, or in the Cr_2O_3 catalyst. This is corroborated by the development of the product concentrations after the introduction of $^{16}O_2$, which is shown in Fig. 4. Quite a few ^{18}O-containing products are formed at the onset of the repeated reaction.

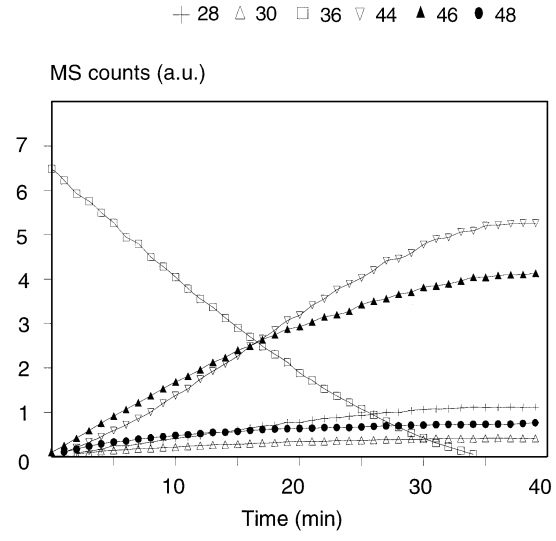

FIG. 4. Development of the $C^{16}O$ (28), $C^{18}O$ (30), $^{16}O_2$ (32), $C^{16}O_2$ (44), $C^{16}O^{18}O$ (46), and $C^{18}O_2$ (48) concentrations in $^{16}O_2$ with time at 675 K. The measurement was performed on a Cr_2O_3/carbon black mixture after treatment of 70-mg sample in $^{18}O_2$ three times.

Furthermore, the development of the $C^{16}O_2$ concentration shows an S-shaped curve, which indicates that a sequential reaction takes place. At the end of this third experiment $C^{16}O_2$ is the main product, followed by $C^{18}O^{16}O$ and $C^{16}O$. The IPR's for the various experiments with the Cr_2O_3 catalyst are shown in Fig. 5. The product ratio calculated after the fourth experiment, which was performed in $^{18}O_2$, is also included. This time, the development of the $C^{18}O_2$ concentration profile showed an S-shaped curve (not shown).

The oxidation patterns obtained for the Fe_2O_3 catalyst are qualitatively similar to the ones presented for the Cr_2O_3 catalyst. However, the Fe_2O_3 catalyst is less active than

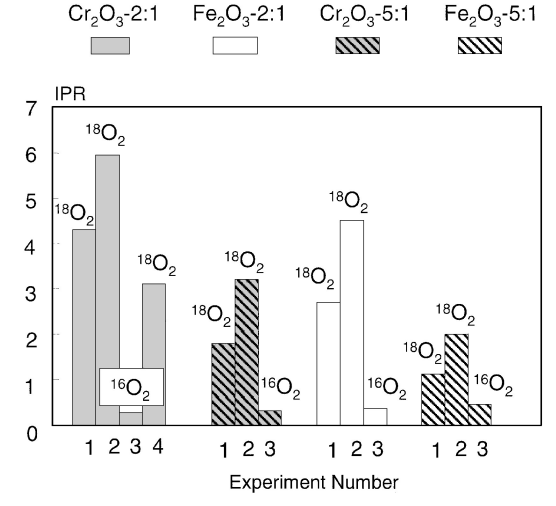

FIG. 5. IPR ratios for Cr_2O_3 and Fe_2O_3 catalyzed carbon black oxidation. Catalyst to carbon black ratios of 2 : 1 and 5 : 1 were applied. The ratios, obtained after experiments performed in $^{16}O_2$, are also shown.

Cr_2O_3, resulting in longer reaction times; 60 min are required to convert 0.3 mbar $^{18}O_2$ at 675 K. The product distributions are included in Fig. 5. The IPRs are somewhat lower than those obtained for the Cr_2O_3 catalyst, but still relatively high. Oxidation of carbon black in the absence of oxygen was not observed; carbothermic reduction of the catalyst does not take place at the experimental conditions. This indicates that surface and/or bulk oxygen are not easily removed from the Fe_2O_3 catalyst.

The isothermal experiment performed in $^{16}O_2$ yielded a similar S-shaped curve for the $C^{16}O_2$ production as was observed for Cr_2O_3. Apparently, the Fe_2O_3 and Cr_2O_3 catalysts behave quite similarly.

Oxidation experiments with samples containing a Cr_2O_3/carbon black and Fe_2O_3/carbon black ratio of 5 : 1, resulted in lower IPRs (Fig. 5) than samples with a 2 : 1 catalyst/carbon black ratio. Apparently, a larger amount of ^{16}O initially associated with the metal oxide is incorporated in the products. The experimental results obtained for $^{16}O_2$ show that a higher IPR is obtained for the 5 : 1 samples in $^{16}O_2$ than for the 2 : 1 samples. This indicates that a larger amount of ^{18}O is incorporated in the 5 : 1 samples than in the 2 : 1 samples. Again, in $^{16}O_2$ S-shaped $C^{16}O_2$ concentration profiles were obtained for both catalysts.

Co_3O_4-Catalyzed Carbon Black Oxidation

The activity of Co_3O_4 in carbon black oxidation is highly dependent on the preparation temperature of the catalyst. Calcination of $Co(NO_3)_2$ at 675 K yields a very active Co_3O_4 catalyst, whereas calcination at higher temperatures (875 K or 1075 K) diminishes the activity (28). In this study, Co_3O_4 prepared by calcination at 875 K was used, because the activity of this catalyst is comparable with the activity of the other catalysts tested. The development of the products formed in $^{18}O_2$ at 625 K, is shown in Fig. 6. The main product is $C^{18}O_2$, followed by $C^{18}O^{16}O$. Contrary to the Fe_2O_3 and Cr_2O_3 samples, changes in the product distribution are observed after complete conversion of $^{18}O_2$; exchange of $C^{18}O_2$ with lattice oxygen yields $C^{16}O^{18}O$ and $C^{16}O_2$. Although the exchange reaction is slower than the oxidation reaction, the influence of this reaction on the calculated IPR is larger for the Co_3O_4 catalyst than for the Cr_2O_3 and Fe_2O_3 catalysts. Besides $C^{18}O_2$ exchange, oxygen exchange between $^{18}O_2$ and Co_3O_4 was also observed, predominantly yielding $^{18}O^{16}O$ (not shown). A very small amount of $^{16}O_2$ was detected, probably formed by a consecutive exchange of $^{18}O^{16}O$ with lattice oxygen. $^{18}O_2$ exchange reactions with lattice oxygen of unsupported transition metal oxides behaved as described in the reviews by Novakova (13), Boreskov (14), and Doornkamp *et al.* (21); they will not be discussed here.

Switching from $^{18}O_2$ to $^{16}O_2$ in a third experiment results in the instant formation of large amounts of ^{16}O-labeled CO and CO_2. An S-shaped curve is not obtained.

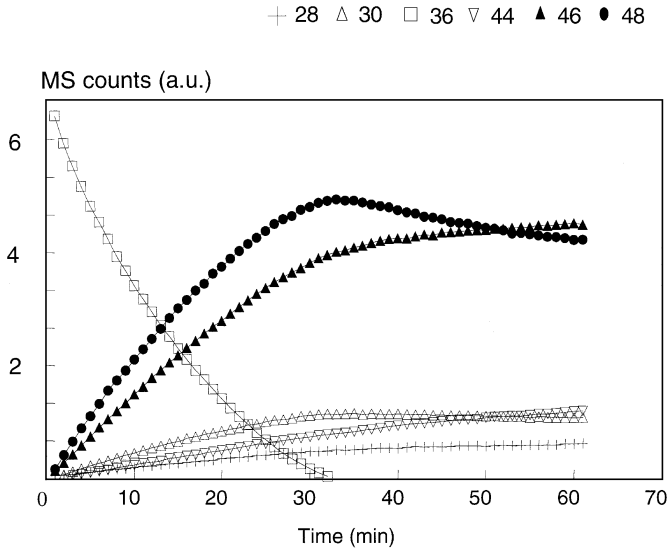

FIG. 6. Development of the $C^{16}O$ (28), $C^{18}O$ (30), $^{18}O_2$ (36), $C^{16}O_2$ (44), $C^{16}O^{18}O$ (46), and $C^{18}O_2$ (48) concentrations in $^{18}O_2$ with time. The measurement was performed on a Co_3O_4/carbon black mixture (2 : 1) after heating 70-mg sample in $^{18}O_2$ to 625 K.

Apparently, only a very small amount of ^{18}O is left in the Co_3O_4/carbon black sample and available for carbon black oxidation. Some of the ^{18}O incorporated in the Co_3O_4 catalyst is exchanged for ^{16}O by reaction with $^{16}O_2$, as gaseous $^{18}O^{16}O$ was detected during the experiment (not shown). An overview of the IPRs obtained for the experiments with the Co_3O_4/carbon black mixture is included in Fig. 7, which contains all results for the 2 : 1 catalyst/carbon black samples.

MoO_3, V_2O_5, and K_2MoO_4 Catalyzed Carbon Black Oxidation

The gas composition evolution for a MoO_3/carbon black sample (in $^{18}O_2$) at 625 K is shown in Fig. 8. A relatively large amount of ^{16}O is incorporated in the products; $C^{18}O^{16}O$ is the main product, followed by $C^{16}O_2$ and $C^{18}O_2$. Hence, it can be concluded that a significant amount of lattice oxygen is involved in the MoO_3 catalyzed carbon black oxidation. The continuous production of $C^{16}O$ is striking because it is nearly independent of the decreasing oxygen partial pressure, indicating a carbothermic reduction of MoO_3. The IPR of the MoO_3/carbon black sample was calculated directly after 100% conversion of the gas phase oxygen (Fig. 7). Experiment 4 (in $^{16}O_2$) shows a relatively high IPR; apparently, during the former three experiments, quite some ^{18}O was incorporated in the MoO_3 lattice, which is available for carbon black oxidation in Experiment 4 (in $^{16}O_2$). In a consecutive experiment in $^{16}O_2$, a much lower IPR is obtained.

The evolution of the gas phase composition for V_2O_5-catalyzed carbon black oxidation in $^{18}O_2$ is shown in Fig. 9. Compared to MoO_3, an even larger amount of $C^{16}O_2$ is formed, indicating a significant participation of lattice oxygen. Although some $C^{16}O_2$ and $C^{16}O$ is produced after complete $^{18}O_2$ conversion, the formation of CO was not as extensive for V_2O_5 as for MoO_3. The $C^{18}O_2$ concentration

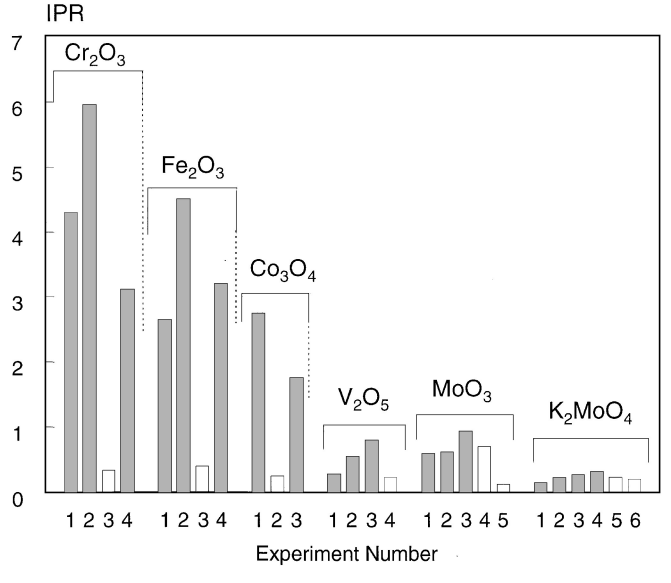

FIG. 7. Development of the IPR ratio with the experiment number for Co_3O_4, MoO_3, V_2O_5, and K_2MoO_4 catalysts. The ratio of Cr_2O_3, and Fe_2O_3 are also shown. A catalyst to carbon black ratio of 2 : 1 was used in all cases. Experiments in $^{16}O_2$ are indicated by an open bar and in $^{18}O_2$ by a solid bar.

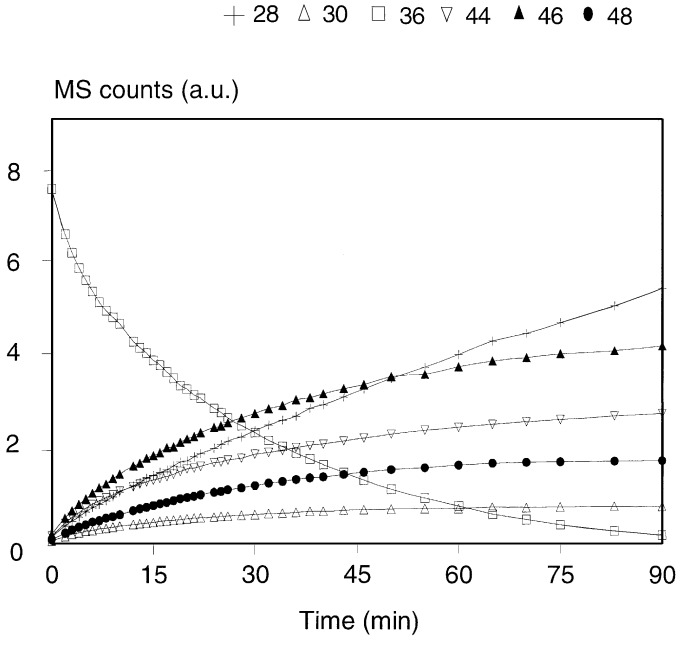

FIG. 8. Development of the $C^{16}O$ (28), $C^{18}O$ (30), $^{18}O_2$ (36), $C^{16}O_2$ (44), $C^{16}O^{18}O$ (46), and $C^{18}O_2$ (48) concentrations in $^{18}O_2$ with time at 625 K. The measurement was performed after heating 70 mg of the MoO_3/carbon black sample (2 : 1) in $^{18}O_2$.

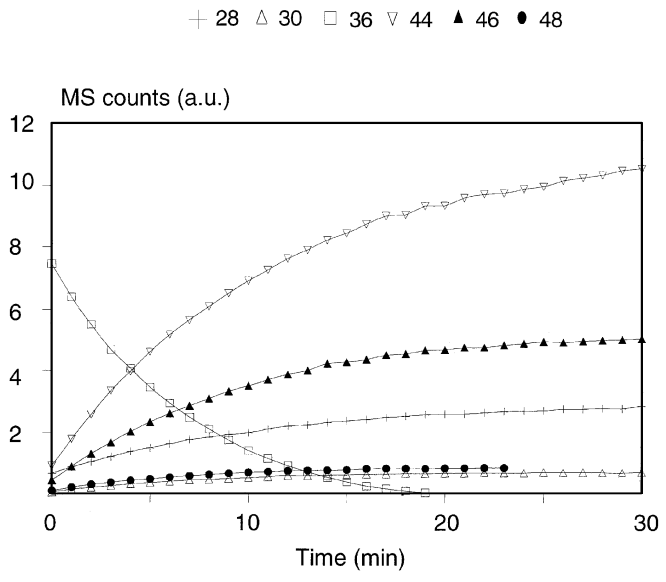

FIG. 9. Development of the $C^{16}O$ (28), $C^{18}O$ (30), $^{18}O_2$ (36), $C^{16}O_2$ (44), $C^{16}O^{18}O$ (46), and $C^{18}O_2$ (48) concentrations in $^{18}O_2$ with time at 625 K, after heating 70 mg of the V_2O_5/carbon black sample in $^{18}O_2$.

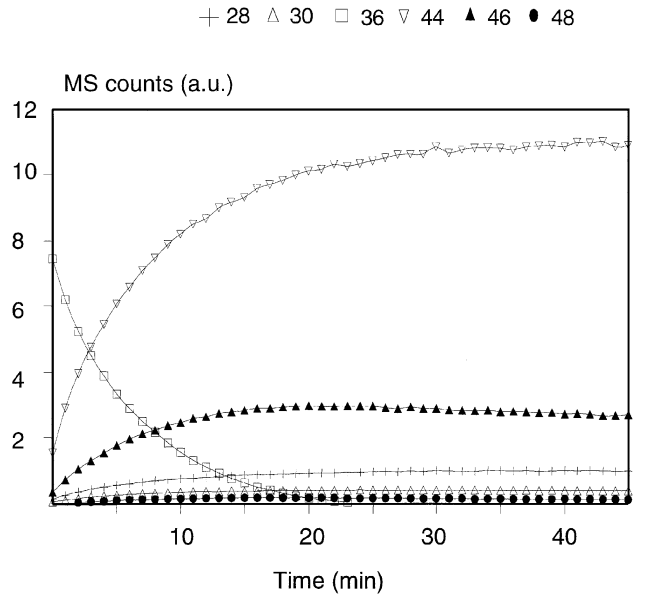

FIG. 10. Development of the $C^{16}O$ (28), $C^{18}O$ (30), $^{18}O_2$ (36), $C^{16}O_2$ (44), $C^{16}O^{18}O$ (46), and $C^{18}O_2$ (48) concentrations in $^{18}O_2$ with time at 625 K, after heating 70 mg of the K_2MoO_4/carbon black sample in $^{18}O_2$.

remained constant after 100% conversion of labeled oxygen, so no oxygen exchange between $C^{18}O_2$ and V_2O_5 takes place. The V_2O_5/carbon black sample was treated three sequential times in $^{18}O_2$, followed by two times in $^{16}O_2$ (Fig. 7). Similar to the MoO_3/carbon black sample, a gradually increasing IPR is observed in consecutive experiments in $^{18}O_2$. In $^{16}O_2$ several ^{18}O-labeled products were detected, although not as much as for MoO_3.

The evolution of the gas phase composition for a K_2MoO_4/carbon black sample in $^{18}O_2$ at 625 K is shown in Fig. 10. Hardly any CO is formed. The major CO_2 product formed is $C^{16}O_2$, followed by $C^{18}O^{16}O$, and a very low amount of $C^{18}O_2$. After 100% conversion of gas phase oxygen, CO and CO_2 are no longer formed. This is in agreement with TG/DSC experiments (35) which indicate that carbothermic (bulk) reduction of K_2MoO_4 is not possible. Furthermore, the oxygen exchange of $C^{18}O^{16}O$ with lattice oxygen occurs at a slow rate, as is witnessed by the concentration development of $C^{18}O^{16}O$ after 100% $^{18}O_2$ conversion. The isothermal reaction of the K_2MoO_4/carbon black mixture was performed four sequential times in $^{18}O_2$, for which the IPR hardly changed (Fig. 7). Correspondingly, in subsequent experiments in $^{16}O_2$ only a very low amount of ^{18}O labeled products was obtained. Isotopic scrambling of the products, as was observed for the Co_3O_4 catalyst, occurs at a lower rate for K_2MoO_4.

DISCUSSION

Overview of the Investigated Catalysts

Table 1 shows an overview of the reaction phenomena observed for the catalysts in the carbon black oxidation in this and other studies (28,30,35). This includes the formation of carbon surface oxygen complexes (SOCs), oxidation of the carbon black by surface and bulk oxygen of the oxides, carbothermic reduction, and oxygen exchanges between the CO/CO_2 products mutually and/or the oxides. The number of +'s indicates a qualitative impression of the relative importance in the behaviour of the different oxides. A − sign indicates that this phenomenon was not observable under the applied conditions.

The formation of SOCs has been revealed by a DRIFT spectroscopic study (28). Except for Fe_2O_3 and Co_3O_4 the catalysts lead to the formation of SOCs. Direct uncatalyzed oxidation by oxygen can be neglected here. This formation

TABLE 1

Reaction Phenomena in the Oxygen-Catalyst-Carbon Black System Observed under the Conditions in This Study

Catalyst	SOCs formation[a] (27)	Carbon oxidation by: Surface oxygen	Carbon oxidation by: Bulk oxygen	Carbothermic reduction[b]	Oxygen exchanges CO/CO_2 and catalyst
Cr_2O_3	++	++	−	−	−
Fe_2O_3	−	++	−	−	−
Co_3O_4	−	+++	−	−	+
MoO_3	++	+	++	++	−
V_2O_5	+	+	+++	++	−
K_2MoO_4	+	+	++++	−	+/−

[a] As observed by DRIFT spectroscopy (28)

[b] As observed in this study; bulk reduction of Fe_2O_3, Co_3O_4, MoO_3, and V_2O_5 was observed at higher temperatures (28).

of SOCs is ascribed to a spill-over of activated oxygen from the catalyst to the carbon surface (28). Therefore, this aspect does not play a role for Fe_2O_3 and Co_3O_4.

The oxides can further interact directly with the carbon black at locations of direct contact through a transfer of oxygen, reducing the oxide locally. The vacancies thus created can be refilled by gas phase oxygen or by oxygen from the surface or the bulk of the oxide. If in the labelling experiments a high IPR is observed this implies that mainly gas phase oxygen is incorporated in the products. An extensive exchange of gas phase oxygen with the oxide surface or with the bulk phase would lead to decreasing IPR values. The absence of carbothermic reduction under the applied conditions and the high IPR values indicate that only surface oxygen is involved in the carbon black oxidation by Fe_2O_3 and Co_3O_4. For Cr_2O_3 another mechanism seems to be involved in view of the SOC formation and the significantly different shape of the isothermal oxidation profile, i.e. rate versus carbon conversion (28,29,36). A spill-over mechanism would lead to high IPR values, as observed. The IPR for Cr_2O_3 and Fe_2O_3, however, both decrease with increasing catalyst/carbon ratio of the sample and, correspondingly, a higher IPR for this higher ratio is found for a subsequent experiment in $^{16}O_2$. This indicates that also for Cr_2O_3 ^{18}O is stored in the catalyst which is involved in the oxidation of the carbon black. The exchange of oxygen between the products and the oxide can be ruled out as an explanation for these two samples, in view of the nearly unchanging isotopic product composition after 100% $^{18}O_2$ conversion. So, although Cr_2O_3 cannot be carbothermally reduced below 1000 K (30,35), oxygen associated with its surface is involved in the carbon black oxidation. Oxygen associated with the surface of Co_3O_4 is also likely to be the only oxygen involved in carbon black oxidation. The IPR would have been higher than the ratio shown in Fig. 10 if oxygen exchange in O_2 and CO_2 had not affected the product distribution.

The oxidation behavior of MoO_3 is different from Fe_2O_3, Co_3O_4, and Cr_2O_3. The IPR values are much smaller. Clearly, for MoO_3 bulk oxygen plays an important role in the reaction with carbon black. The predominant formation of $C^{16}O$ is probably induced by evaporation and sublimation processes occurring under the reaction conditions (675 K, high vacuum). MoO_3 is known to have a rather high vapor pressure at relatively low temperatures (37). The reaction of the sublimed oxide with carbon black yields CO and MoO_2. Since the reaction is stoichiometric and MoO_2 is not carbothermically reduced further at 675 K, CO_2 is not formed. The relatively higher IPR for the first measurement in $^{16}O_2$ (Fig. 7) suggests that scrambling of ^{18}O with bulk lattice oxygen in MoO_3 occurs to a lesser extent than for V_2O_5 and K_2MoO_4. This might be related to the above-mentioned sublimation. So, besides a proposed spill-over mechanism, witnessed by SOC formation in DRIFT spectroscopic observations (28), lattice (bulk) oxygen of MoO_3 is participating in the catalytic oxidation of carbon black.

Some $C^{16}O_2$ and $C^{16}O$ is produced after 100% $^{18}O_2$ conversion for V_2O_5. A DRIFT spectrum of the V_2O_5/carbon black sample, recorded after the oxidation experiments (not shown) revealed the formation of reduced vanadium species. Hence, carbothermic reduction of V_2O_5 did occur and lattice oxygen of V_2O_5 is participating in the catalytic oxidation of carbon black, explaining the product distributions for this catalyst (28). Our results do not suggest oxygen exchange reactions between products mutually or with the oxide as it has been observed for MoO_3 and V_2O_5 (38). This indicates that the carbon oxidation rates over these oxides are much faster than these exchange reactions.

The catalysis by K_2MoO_4 is rather unique in the sense that hardly any gas-phase oxygen is directly incorporated in the oxidation products. Although $^{18}O_2$ exchange rates are not available for this compound, a very fast and efficient oxygen exchange with the bulk of the oxide must occur at the reaction conditions applied. The large amount of ^{16}O present in the sample, relative to gas phase $^{18}O_2$, results in a nearly quantitative incorporation of ^{18}O in the K_2MoO_4 lattice, and the release of mainly ^{16}O labeled products. The oxygen exchange between $C^{18}O_2$ and lattice oxygen has also been considered, but was hardly observed in the absence of $^{18}O_2$ (Fig. 9). The present study and a separate TG/DSC analysis (35) have shown that carbothermic reduction of K_2MoO_4 does not occur. Thus, gas phase oxygen is required for the formation of gaseous carbon oxides.

In general the results obtained for the metal oxides investigated can be correlated to the reducibility and mobility (or exchangeability) of lattice oxygen. The amount of bulk or lattice oxygen incorporated in the oxidation products decreases in the sequence $K_2MoO_4 > MoO_3 > V_2O_5 > Co_3O_4 = Fe_2O_3 > Cr_2O_3$. This range corresponds well with literature dealing with $^{18}O_2$ exchange reactions: less than one monolayer is exchangeable for Co_3O_4, a monolayer for γ-Fe_2O_3 and α-Cr_2O_3, and the entire bulk for MoO_3 and V_2O_5 (14–16). The mobility of lattice oxygen ions in MoO_3 and V_2O_5 is rather high. Therefore, quite some ^{18}O can be absorbed by these metal oxides, yielding ^{16}O-labeled carbon oxide species. The observed low IPR ratio for V_2O_5 and MoO_3 can thus be explained. The results for K_2MoO_4 suggest an even higher mobility of lattice oxygen.

Oxidation Mechanism

The experimental results presented here and the formation of surface oxygen complexes (28) can be explained if three types of oxygen are defined for the oxides: *adsorbed*-surface oxygen, surface oxygen, and lattice (or bulk) oxygen. *Adsorbed*-surface oxygen is defined as activated oxygen located **on** the surface of a metal oxide (it is not

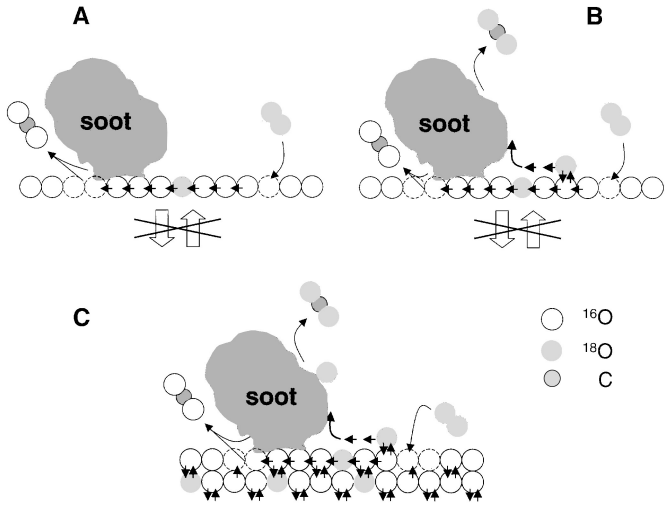

FIG. 11. The processes occurring on the surfaces of different transition metal oxides: (A) Co_3O_4 and Fe_2O_3; (B) Cr_2O_3; (C) MoO_3, V_2O_5, and K_2MoO_4. Active sites (vacancies) are indicated by squares, and lattice oxygen ions by circles. Charge transfers are not considered.

incorporated in the surface layer). These oxygen species might migrate over the oxide surface or spill-over to the carbon black. Surface oxygen is activated oxygen which is incorporated **in** the surface (i.e., the first oxygen layer) and transported via the surface to the catalyst/carbon black interface. Lattice oxygen is defined as oxygen associated with the bulk of the metal oxide, below surface oxygen. An overview of the interactions of oxygen species with the metal oxides, based on the experimental results summarized in Table 1, is given in Fig. 11.

Model A in Fig. 11 represents a modified Mars and van Krevelen mechanism, valid for Fe_2O_3 and Co_3O_4 catalysis. First, ^{16}O atoms react at the catalyst/carbon black interface to CO/CO_2 and are replaced by ^{16}O atoms, initially present in the surface layer of Fe_2O_3 and Co_3O_4. Simultaneously, ^{18}O atoms are generated at vacancies and incorporated in the surface layer of the metal oxide. These ^{18}O atoms become identical to the ^{16}O atoms and can be transported through the surface metal oxide surface layer to the catalyst/carbon black interface. Finally, the ^{18}O atoms react at the surface/carbon black interface. The experimental results suggest that the reaction of surface oxygen with carbon black is only possible if gas phase oxygen is present. Apparently gas phase oxygen is needed to activate surface oxygen, i.e. to maintain a surface oxygen concentration gradient (or chemical potential gradient) to "push the chain of surface oxygen atoms" forward to the metal oxide/carbon black interface. A slight surface reduction causes stagnation of this chain, as the residual surface oxygen is more strongly bound, due to oxygen deficiency in this layer. A more complex description of the processes occurring on the Cr_2O_3 surface is needed to explain all the experimental observations (Fig. 11, model B). Besides surface oxygen, several ^{18}O atoms are not incorporated into the Cr_2O_3 surface layer but are assumed to be present as activated *adsorbed* surface oxygen species which move in an activated state over the surface (indicated by an asterisk) to a carbon black particle, spill-over, and form SOCs. These complexes slowly decompose yielding ^{18}O-labeled carbon oxides. Whether exchange of $^{18}O^*$ with surface ^{16}O can occur before SOCs are formed, remains to be elucidated. Combining the exchange of bulk oxygen with surface oxygen with the mechanism for the Cr_2O_3, yields the proposed oxidation model for V_2O_5 and MoO_3 (Fig. 11, model C). Also for these oxides, *adsorbed* surface oxygen might spill-over onto the carbon surface, yielding SOCs. Furthermore, surface oxygen is exchanged with bulk oxygen, explaining the low IPR ratio for these catalysts. Gas phase oxygen is not needed to "push the chain forward"; transport of bulk oxygen atoms to the catalyst/carbon black interface occurs in the absence of gas phase oxygen, as is witnessed by carbothermic reduction.

The reaction of potassium-containing catalysts with carbon has been studied extensively by Cerfontain and Moulijn (39,40) and Meijer *et al.* (41,42). A potassium oxide cluster is proposed as being the active species. DRIFT spectroscopy and X-ray diffraction have shown that potassium oxide clusters might very well be formed by disproportionation of K_2MoO_4, yielding K_2O and $K_2Mo_2O_7$ (35). Furthermore, a rather strong interaction of potassium ions with carbon oxygen complexes has been found (35). From the observations made, the so-called push-pull mechanism (see the Introduction of this paper) is proposed for K_2MoO_4; a simultaneous reduction and reoxidation of an active site, followed by oxygen exchange with the bulk, can explain the experimental results. In fact this mechanism is quite similar to scheme C of Fig. 11, with the exception that bulk oxygen does not react in the absence of gas phase oxygen: the "oxygen chain", including the bulk, can only be pushed forward in the presence of oxygen.

In summary, the interplay between surface and lattice oxygen of metal oxides determines to a great extent the final product distributions in carbon oxidation: the higher the exchange rate of gas phase and surface oxygen with the bulk, the smaller the amount of oxygen, originating from the gas phase, incorporated in the products. It is emphasized that the processes observed under the test conditions presented do not necessarily occur under real diesel exhaust conditions. The investigations described in this paper were conducted with samples where the carbon black and the catalyst were in very close proximity ("tight contact"). The conditions in ceramic catalytic soot filters are such that only a very poor contact between the catalyst and soot (carbonaceous material) exists ("loose contact"). In this situation, the contribution of lattice and surface oxygen to the oxidation mechanism seems less important, whereas spill-over oxygen might play a more predominant role. In fact, Fe_2O_3 and Co_3O_4 completely lose their carbon oxidation activity

under loose contact conditions, whereas Cr_2O_3, MoO_3, and V_2O_5 show continuing activity. Besides spill-over oxygen, spreading of the catalyst or "wetting" of the carbon black also is an important parameter determining loose contact activity, as has been discussed elsewhere (43–45).

CONCLUSIONS

Three oxidation mechanisms are proposed to occur in the catalyzed carbon black oxidation: a redox mechanism, involving surface or lattice oxygen associated with the metal oxide; a spill-over mechanism, involving adsorbed surface oxygen yielding carbon surface oxygen complexes; and a push-pull mechanism. Lattice oxygen of Cr_2O_3, Fe_2O_3, and Co_3O_4 is hardly involved in the catalytic oxidation of carbon black. Only reduction and reoxidation of the surface layer is likely to occur. In the case of Cr_2O_3, *adsorbed* surface oxygen is to a certain extent also involved in the oxidation.

Quite some lattice oxygen of V_2O_5 and MoO_3 is incorporated in the carbon oxides produced. Moreover, V_2O_5 and MoO_3 are carbothermally reduced in the absence of $^{18}O_2$, yielding $C^{16}O_2$ and $C^{16}O$. MoO_3 yields relatively high amounts of $C^{16}O$, explained by carbothermic reduction of evaporated MoO_3 species to MoO_2. *Adsorbed* surface oxygen is likely to be involved in the oxidation mechanism, but hardly contributes to the isotopic product distributions obtained in this study. In K_2MoO_4 catalyzed carbon black oxidation a simultaneous reduction and reoxidation via a push-pull mechanism takes place, accompanied by a fast oxygen exchange with bulk oxygen.

ACKNOWLEDGMENTS

The authors acknowledge the fruitful discussions with Professor Dr. V. Ponec, Leiden University, The Netherlands. The research has been supported by the Netherlands Foundation for Chemical Research (SON) with financial aid from the Netherlands Organization for Scientific Research (NWO) and under the auspices of NIOK, the Netherlands Institute for Catalysis, Publication TUD 98-4-853.

REFERENCES

1. Kröger, C., *Z. Anorg. Allg. Chem.* **206**, 289 (1932).
2. Mars, P., and Van Krevelen, D. W., *Chem. Eng. Sci.* **3**, 41 (1954).
3. Sokolovskii, V. D., *Catal. Rev.-Sci. Eng.* **32**, 1 (1990).
4. Bielanski, A., and Haber, J., "Oxygen in Catalysis," Dekker, New York, 1991.
5. Golodets, G. I., *Stud. Surf. Sci. Catal.* **15**, 438 (1983).
6. Maltha, A., Van Wermeskerken, S. C., Favre, T. L. F., Angevaare, P. A. J. M., Grootendorst, E. J., Koutstaal, C. A., Zuur, A. P., and Ponec, V., *Catal. Today* **10**, 387 (1991).
7. Weng, L. T., Ruiz, P., Ma, Y., and Delmon, B., *J. Mol. Catal.* **61**, 99 (1990).
8. Weng, L. T., Ruiz, P., and Delmon, B., *Stud. Surf. Sci. Catal.* **72**, 399 (1992).
9. Weng, L. T., Ruiz, P., and Delmon, B., *J. Mol. Catal.* **52**, 349 (1989).
10. Winter, E. R. S., *J. Chem. Soc.* 2726 (1955).
11. Winter, E. R. S., *J. Chem. Soc.* 5781 (1964).
12. Winter, E. R. S., *J. Chem. Soc. A*, 2889 (1968).
13. Novakova, J., *Catal. Rev.* **4**, 77 (1970).
14. Boreskov, G. K., *Adv. Catal.* **15**, 285 (1964).
15. Popovskii, V. V., Boreskov, G. K., Muzykantov, V. S., Sazonov, V. A., and Shubnikov, S. G., *Kinet. Katal.* **10**, 643 (1969).
16. Muzykantov, V. S., Cheshkova, T., and Boreskov, G. K., *Kinet. Katal.* **14**, 365 (1973).
17. Keulks, G. N., *J. Catal.* **19**, 232 (1970).
18. Iizuka, Y., *J. Chem. Soc., Faraday Trans.* **90**, 1301 (1994).
19. Iizuka, Y., Tanigaki, H., Sanada, M., Tsunetoshi, J., Yamauchi, N., and Aral, S., *J. Chem. Soc., Faraday Trans.* **90**, 1307 (1994).
20. Iizuka, Y., Tsunetoshi, J., Yamauchi, N., and Aral, S., *J. Chem. Soc., Faraday Trans.* **90**, 3449 (1994).
21. Doornkamp, C., Clement, M., and Ponec, V., *J. Catal.*, in press.
22. Kyotani, T., Hayashi, S., and Tomita, A., *Energy Fuels* **5**, 683 (1991).
23. Kyotani, T., Hayashi, S., Tomita, A., MacPhee, J. A., and Martin, R. R., *Fuel* **71**, 655 (1991).
24. Martin, R. R., MacPhee, J. J., Kyotani, T., Hayashi, S., and Tomita, A., *Carbon* **29**, 475 (1991).
25. Serra, V., Saracco, G., Badini, C., and Specchia, V., *Appl. Catal. B: Env.* **11**, 329 (1997).
26. McKee, D. W., *Fuel* **62**, 170 (1983).
27. McKee, D. W., *J. Catal.* **108**, 480 (1987).
28. Mul, G., Neeft, J. P. A., Kapteijn, F., and Moulijn, J. A., *Carbon* **36**, 1269 (1998).
29. Neeft, J. P. A., Makkee, M., and Moulijn, J. A., *Fuel* **77**, 111 (1998).
30. Baker, R. T. K., and Chludzinski, J. J., *Carbon* **19**, 75 (1981).
31. Van Doorn, J., Varloud, J., Meriaudeau, P., and Perrichon, V., *Appl. Catal. B: Env.* **1**, 117 (1992).
32. Mestl, G., Herzog, B., Schloegl, R., and Knözinger, H., *Langmuir* **11**, 3027 (1995).
33. Mestl, G., Verbruggen, N. F. D., and Knözinger, H., *Langmuir* **11**, 3035 (1995).
34. Grootendorst, E. J., "Selective Reduction Reactions on Oxidic Catalysts," Ph.D. thesis, Leiden University, 1994.
35. Mul, G., Kapteijn, F., and Moulijn, J. A., A DRIFTS study of the interaction of alkali metal oxides with carbonaceous surfaces, *Carbon*, in press.
36. Mul, G., Kapteijn, F., and Moulijn, J. A., *in* "Proceedings of 22nd Biennial Conference on Carbon, San Diego, 1995," p. 554.
37. Knacke, O., Kubachewski, O., and Hesselman, K., "Thermochemical Properties of Inorganic Substances," Springer-Verlag, Berlin, 1991.
38. Boreskov, G. K., and Muzykantov, V. S., *Ann. N. Y. Acad. Sci.* **213**, 137 (1973).
39. Cerfontain, M. B., and Moulijn, J. A., *Fuel* **62**, 256 (1983).
40. Cerfontain, M. B., and Moulijn, J. A., *in* "Proc. Int. Conf. Coal Science, 1983," p. 419.
41. Meijer, R., Van der Linden, B., Kapteijn, F., and Moulijn, J. A., *Fuel* **70**, 205 (1991).
42. Meijer, R., Kapteijn, F., and Moulijn, J. A., *Fuel* **73**, 723 (1994).
43. Oh, S. G., and Baker, R. T. K., *J. Catal.* **128**, 137 (1991).
44. Mul, G., Kapteijn, F., and Moulijn, J. A., *Appl. Catal. B: Env.* **12**, 33 (1997).
45. Neeft, J. P. A., Makkee, M., and Moulijn, J. A., *Appl. Catal. B: Env.* **8**, 57 (1996).